p s s physica status solidi a
www.pss-a.com

applications and materials science

Three-step growth method for high quality AlN epilayers

M. L. Nakarmi*[,1,2], B. Cai[1,2], J. Y. Lin[3], and H. X. Jiang[3]

[1] Department of Physics, Brooklyn College of the City University of New York, Brooklyn, NY 11210, USA
[2] Graduate Center of the City University of New York, New York, NY 10031, USA
[3] Department of Electrical and Computer Engineering, Texas Tech University, Lubbock, TX 79409, USA

* Corresponding author: e-mail mlnakarmi@brooklyn.cuny.edu, Phone: +1-718-9515148, Fax: +1-718-9514407

We report a three-step growth method to grow thick and high quality aluminum nitride (AlN) epilayers on sapphire substrates by metal organic chemical vapor deposition (MOCVD). The three-step growth method begins with a deposition of a thin AlN buffer layer at 950 °C followed by an intermediate AlN (I-AlN) layer at 1100 °C, and finally a thick AlN epilayer at high temperature around 1325 °C. AlN epilayers grown by this method have smooth surfaces, narrow width of X-ray rocking curves, and strong band edge photoluminescence (PL) emissions with low impurity emissions. Transmission electron microscopy revealed that most of the threading dislocations are annihilated within 300 nm. Stacking faults are greatly reduced in epilayers grown by this method resulting in very low screw type threading dislocation density. Dominant threading dislocations in the AlN epilayers are edge type originated from misfit dislocations (MD).

1 Introduction Aluminum nitride (AlN) having a direct band gap of ~6.1 eV, has emerged as a promising deep ultraviolet (DUV) material with the demonstrations of AlN based 210 nm light emitting diodes (LED) and photodetectors with cut off wavelengths of 200 nm [1, 2]. AlN possesses outstanding properties, such as high temperature stability, hardness, and high thermal conductivity, which make it a good candidate for high temperature/power/radiation devices [3]. Because of the piezoelectric property, it has also applications in surface acoustic wave devices [4]. AlN based photonic devices could be efficient and robust due to the large free exciton binding energy and short radiative lifetime [5, 6]. When alloyed with gallium nitride (GaN), AlGaN are the most promising materials for DUV optoelectronic devices operating in the wavelength range shorter than 300 nm [7]. Thus, the growth methods for producing high quality AlN epilayers are widely sought to exploit its outstanding properties in the device applications. High quality AlN epilayers can also be used as templates to grow nitride based device structures.

A two-step growth method developed for the growth of GaN epilayer on sapphire substrate by metal organic chemical vapor deposition (MOCVD) is widely used to grow nitride materials [8, 9]. In the two-step growth method for GaN, a thin buffer layer is grown on the sapphire substrate at low temperature ~550 °C followed by the growth of thick epilayer at high temperature ~1000 °C. The buffer layer is critical in the growth of nitride materials to overcome the problems caused by the large lattice and thermal mismatches with sapphire substrates, and reduce the density of threading dislocations. The growth of AlN has additional problems due to the low surface migration of Al adatoms and parasitic gas reaction between aluminum source and ammonia [10]. High growth temperature and low pressure is thus required for the growth of AlN to provide enough mobility to aluminum adatoms. Various methods are used to improve the material quality of AlN, for example, pulsed growth of AlN [11, 12], use of alternating V/III ratio [13], nitridation of the substrate [14], and epitaxial lateral overgrowth [15]. The growth of thick and low dislocation density AlN epilayer is still difficult.

We have developed a three-step growth method for the growth of high quality AlN epilayers on sapphire substrates by MOCVD. In this paper, we report on the growth process and structural analysis of AlN epilayers grown by the three-step method. The samples were characterized by X-ray diffraction (XRD), atomic force microscopy (AFM), DUV photoluminescence (PL), and transmission electron microscopy (TEM).

WILEY ONLINE LIBRARY

Phys. Status Solidi A **209**, No. 1 (2012)

127

2 Experimental

2.1 Growth by MOCVD The samples were grown on *c*-plane sapphire substrates by MOCVD. The schematic layer structure of AlN epilayers grown by three-step method is shown in the inset of Fig. 1. An intermediate AlN (I-AlN) layer was inserted between the buffer and high temperature AlN (HT-AlN) epilayers. This additional layer is a key difference compared to the conventional two-step method. The growth process started with the thermal cleaning of the substrate in hydrogen ambience prior to the growth in a horizontal reactor. In an optimized growth process, the growth was initiated with a thin AlN buffer layer at 950 °C. An I-AlN of thickness ∼120 nm was then grown at 1100° C. The top HT-AlN was grown at 1325 °C which was limited by the system. Growth pressure throughout the process was 40 Torr. Trimethylaluminum (TMAl) and blue ammonia were used as the aluminum (NH_3) and nitrogen sources, respectively. Hydrogen was used as the carrier gas. The flow rates for TMAl and NH_3 were about 20 mL/min and 2 L/min, respectively. Growth rate of about 1.2 μm/h was obtained under these conditions. AlN epilayers with thickness ranging from 1 to 4 μm were grown without cracks. A typical *in situ* optical reflectance curve of AlN epilayer grown by three-step method is shown in Fig. 1.

A small signal can be seen during the buffer growth. Significant reflectance is observed during the growth of I-AlN and HT-AlN layers. The reflectivity is higher during the growth of the high temperature layer than that of the intermediate layer. Average reflectance intensity is almost constant during the HT-AlN growth indicating a smooth surface. The reflection curve is different from a typical GaN growth process in which the reflectivity drops to its minimum in the beginning of high temperature growth and it recovers as thickness increases [16, 17]. In the AlN growth, we found that if the average reflectance intensity dropped, it is very
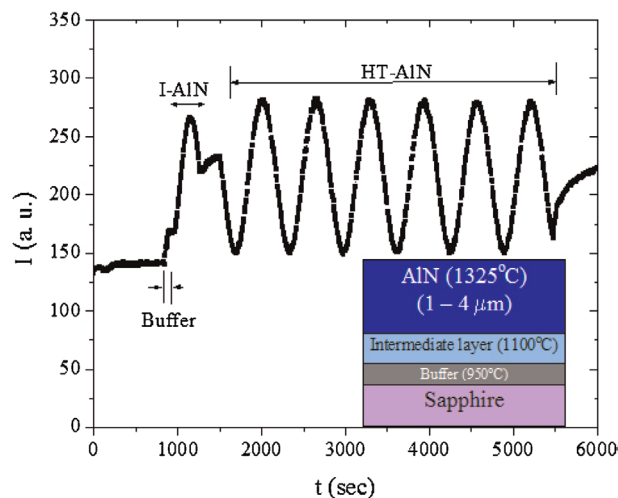
difficult to recover the reflectance signal which ultimately leads to a rough surface. An AlN buffer does not smear by annealing while ramping up the growth temperature as in GaN. Growth of AlN epilayer on sapphire substrates using the two-step method often leads to a rough surface. With the insertion of I-AlN layer between the buffer and HT-AlN layer, a smooth surface is routinely obtained.

3 Results and discussion
Atomic force microscopy images of AlN epilayers showed very smooth surface. The inset of Fig. 2 shows an AFM image with root mean square roughness about 0.5 nm in 1 μm × 1 μm scan size. With the insertion of I-AlN layer, the band edge (impurity) emission intensity in PL measurement has significantly increased (decreased) in our samples. A typical room temperature PL spectrum of AlN epilayer grown by the three-step method is shown in Fig. 2. The samples have a strong band edge emission peak at 5.98 eV with very low impurity emissions at room temperature, ensuring excellent optical quality of the material. At 10 K, the band edge emission peak is at 6.06 eV. Detailed optical properties of AlN epilayers grown on sapphire substrates are also reported elsewhere [2, 5, 18–20].

The full width at half maximum (FWHM) of XRD rocking curves of the (0002) and ($10\bar{1}2$) reflection planes were 63 and 437 arcsec, respectively, for AlN epilayer of thickness 4 μm, and XRD analysis was reported elsewhere [21].

In order to investigate the growth process of AlN epilayers grown by the three-step method, TEM samples for both cross-section and plan view TEM imaging were prepared. The TEM samples were prepared by using Fischione ultrasonic disk cutter, mechanical grinding, and polishing followed by dimple grinding, and Ar^+ ion milling. The TEM characterization was carried out using a JEOL 2010 TEM system operating at 200 kV. Figure 3 shows a typical bright field plan view TEM image of an AlN epilayer taken with $g = 11\bar{2}0$ with the specimen tilted at ∼18° from [0001] zone axis. All three types of dislocations – edge, screw, and mixed can be detected by tilting the sample in the

Figure 1 (online color at: www.pss-a.com) A typical *in situ* optical reflection curve during the growth of AlN epilayer by three-step method. Inset: Schematic layer structure of three-step growth method. An intermediate AlN (I-AlN) layer is inserted between the buffer and high temperature layer.
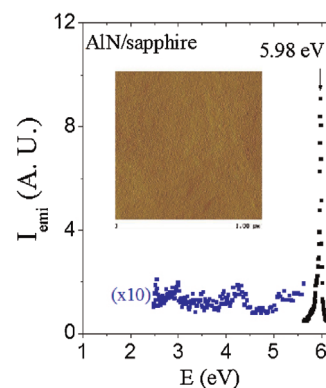

Figure 2 (online color at: www.pss-a.com) PL spectrum of AlN epilayers grown on sapphire substrates measured at room temperature. Inset is the AFM image taken in 1 μm × 1 μm scan size. Rms surface roughness is about 0.5 nm.
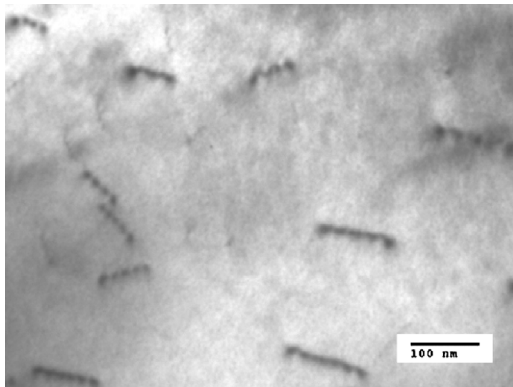
Figure 3 Bright field plan view TEM images of AlN epilayer taken with $g = 11\bar{2}0$ and tilted at $18\,^\circ$ from [0001] zone axis.

plan view image using $g = 11\bar{2}0$ [22]. Here it should be noted that the dominant threading dislocations observed are edge type. The screw and the mixed dislocations were seldom observed. Based on the plan view images the average total dislocation density is $\sim 2 \times 10^9\,cm^{-2}$. Our results agree well with the dislocation densities estimated from the analysis of XRD rocking curves [21].

Figure 4a shows a representative bright field cross-section TEM image of an AlN epilayer sample. The image was taken near zone axis $[2\bar{1}\,\bar{1}0]$. Threading dislocations are generated at the interface of AlN and sapphire. We did not observe distinct interfaces of the intermediate layer and high temperature layer. The dotted line in the Fig. 4a indicates the
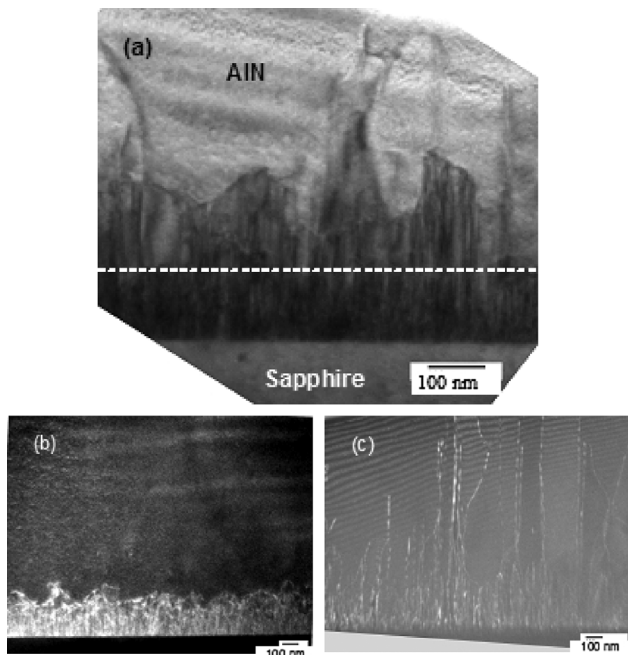

Figure 4 (a) Bright field cross-section view TEM image of AlN epilayer taken near zone axis $[2\bar{1}\,\bar{1}0]$. (b) Dark field cross-section TEM image under two beam condition with $g = 0001$ and (c) dark field cross-section TEM image under two beam condition with $g = 1\bar{1}00$.

region where the growth of HT-AlN starts. In the beginning of HT-AlN growth, the threading dislocations start bending and annihilating. From the TEM images, we observed that most of the threading dislocations are annihilated within the thickness of ~ 300 nm. Figure 4b and c shows the dark field cross-section images taken with $g = 0001$ and $1\bar{1}00$, respectively. Under the two-beam condition ($\boldsymbol{g} \cdot \boldsymbol{b}$), screw and edge type threading dislocations with Burgers vectors $\boldsymbol{b} = \langle 0002 \rangle$ and $\boldsymbol{b} = 1/3 < 1\bar{2}10 >$ are visible with $g = 0001$ and $1\bar{1}00$, respectively [23, 24]. Although dislocations can be seen in the beginning of the growth, they annihilate, leaving the screw type threading dislocation almost clean in the HT-AlN region as shown in Fig. 4b. Edge type threading dislocations are dominant as shown in Fig. 4c. This is consistent with the plan view TEM images with dominant edge type threading dislocations. The edge type threading dislocations are annihilated as the thickness increased forming loops. However, some dislocations propagate vertically.

Figure 5 shows a high resolution TEM image taken near zone axis $[2\bar{1}\,10]$ near the interface of AlN and sapphire substrate. At the interface of AlN and sapphire, the contrast modulations due to the strain near misfit dislocations (MD) can be observed. It is believed that the formation of periodic arrays of MD is due to the slip causing strain relaxation in the region without threading dislocations [25]. Some regions the strain is relaxed by generating threading dislocations. In the high resolution cross-section image, well-aligned basal planes can be clearly observed indicating very low staking fault. The reduced staking fault is consistent with the small FWHM of XRD rocking curve measured at symmetric peak at (0002). Screw dislocations are normally generated from the stacking faults tilting the symmetric planes which broaden the FWHM of rocking curves measured at symmetric planes such as (0002) plane [26].

The AlN structure has the highest stacking fault energy among all nitride-based wurtize materials [27]. We found that AlN epilayers grown with buffer temperature around $950\,^\circ C$ have much smaller FWHM of XRD rocking curve measured at symmetric peak at (0002) compared to the samples grown with buffer temperature around $550\,^\circ C$ (GaN reference). Similar results were reported for AlN directly

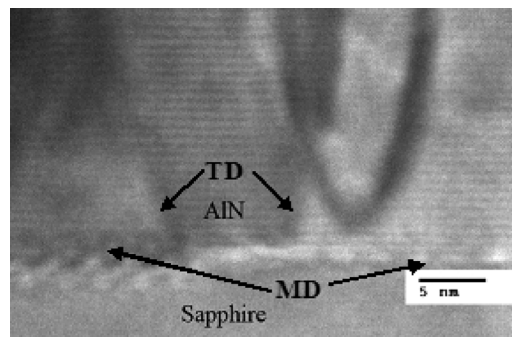**Figure 5** High resolution cross-section TEM image taken near zone axis $[2\bar{1}\,10]$ near the interface of AlN and sapphire substrate.

Phys. Status Solidi A **209**, No. 1 (2012)

Original

Paper

129

grown on sapphire substrate using high temperature growth condition [28]. However, the FWHM of rocking curves measured at asymmetric plane $(10\bar{1}2)$ are normally more than one order in magnitude larger than the FWHM measured at symmetric plane (0002). FWHM of rocking curves measured at asymmetric planes such as $(10\bar{1}2)$ plane are related to the density of edge dislocations [26]. AlN epilayers grown on sapphire substrate thus, suffer from the large density of edge dislocations. Edge type threading dislocations are generated mainly from MD due to the intrinsic lattice mismatch of AlN with sapphire. Reducing edge type threading dislocations is a major challenge in AlN growth. Edge type threading dislocations can be reduced by annihilation by forming a loop with similar neighboring dislocations having opposite Burger vectors [29].

We believe that three-dimensional island growth dominates in buffer and two-dimensional growth dominates in HT-AlN. The transition from three-dimensional to two-dimensional growth occurs during the growth of I-AlN. This layer promotes bending of the propagation and annihilation of threading dislocations during the growth. We found that the thicknesses of the buffer and I-AlN layers are critical for reducing FWHM of rocking curves measured at $(10\bar{1}2)$ planes and hence edge dislocation density. Threading dislocations with large deviation angles annihilated faster whereas threading dislocations with small deviation angles annihilate forming large loops as thickness was increased. The use of high temperature buffers and insertion of I-AlN promote bending of threading dislocations in various angles (as high as 45° from the growth direction), and releasing the strain induced by lattice and thermal mismatch. This could be the reason that we could grow thick AlN epilayers up to 4 μm without any cracks. Threading dislocation density could be further reduced by using higher growth temperature for HT-AlN layer [6]. The three-step method could be transferred to grow AlN epilayers on other substrates and other growth techniques.

4 Conclusion We have developed a three-step method to grow thick and high quality AlN epilayers on sapphire substrates by MOCVD. The three-step method has an I-AlN layer grown at 1100 °C between the buffer grown at 950 °C and HT-AlN at 1325 °C. The AlN epilayers grown by three-step method have a smooth surface and a strong band edge PL emission with low impurity emissions. TEM images revealed that the stacking fault is greatly reduced in AlN epilayers grown by this method leading to extremely low screw type threading dislocation density. Dominant threading dislocations are edge type which is originated from MD.

References

 [1] Y. Taniyasu, M. Kasu, and T. Makimoto, Nature (London) **441**, 325 (2006).

 [2] J. Li, Z. Y. Fan, R. Dahal, M. L. Nakarmi, J. Y. Lin, and H. X. Jiang, Appl. Phys. Lett. **89**, 213510 (2006).

 [3] O. Madelung, Semiconductor – Basic Data (Springer, New York, 1996), p. 69.

 [4] E. Levinshtein, S. L. Ramyantev, and M. S. Shur, Properties of Advanced Semiconductor Materials (Wiley, New York, 2001), p. 31.

 [5] B. Nam, J. Li, M. L. Nakarmi, J. Y. Lin, and H. X. Jiang, Appl. Phys. Lett. **82**, 1694 (2003).

 [6] T. Onuma, K. Hazu, A. Uedono, T. Sota, and S. F. Chichibu, Appl. Phys. Lett. **96**, 061906 (2010).

 [7] A. Khan, Phys. Status Solidi A **203**, 1764 (2006).

 [8] H. Amano, N. Sawaki, I. Akasaki, and Y. Toyoda, Appl. Phys. Lett. **48**, 353 (1986).

 [9] S. Nakamura and G. Fassol, The Blue Laser Diode (Springer, New York, 1997).

[10] T. Uchida, K. Kusakabea, and K. Ohkawa, J. Cryst. Growth **304**, 133 (2007).

[11] M. Asif Khan, J. N. Kuznia, R. A. Skogman, D. T. Olson, M. Mac Millan, and W. J. Choyke, Appl. Phys. Lett. **61**, 2539 (1992).

[12] A. Chitnis, J. P. Zhang, V. Adivarahan, M. Shataloov, S. Wu, R. Pachipulusu, V. Mandavilli, and M. A. Khan, Appl. Phys. Lett. **82**, 2565 (2003).

[13] M. Imura, N. Fujimoto, N. Okada, K. Balakrishnan, M. Iwaya, S. Kamiyama, H. Amano, I. Akasaki, T. Noro, T. Tagaki, and A. Bandoh, J. Cryst. Growth **300**, 136 (2007).

[14] Q. Paduano and D. Weyburne, Jpn. J. Appl. Phys. **42**, 1590 (2003).

[15] M. Imura, K. Nakano, T. Kitatano, G. Narita, N. Okada, K. Balakrishnan, M. Iwaya, S. Kamiyama, H. Amano, I. Akasaki, K. Shimono, T. Noro, and T. Takagi, Appl. Phys. Lett. **89**, 221901 (2006).

[16] J. Han, T.-B. Ng, R. M. Biefeld, M. H. Crawford, and D. M. Follstaedt, Appl. Phys. Lett. **71**, 3114 (1997).

[17] D. G. Zhao, J. J. Zhu, Z. S. Liu, S. M. Zhang, H. Yang, and D. S. Jiang, Appl. Phys. Lett. **85**, 1499 (2004).

[18] J. Li, K. B. Nam, M. L. Nakarmi, J. Y. Lin, H. X. Jiang, P. Carrier, and S.-H. Wei, Appl. Phys. Lett. **83**, 5163 (2003).

[19] N. Nepal, K. B. Nam, J. Li, J. Y. Lin, and H. X. Jiang, Proc. SPIE **5725**, 119 (2005).

[20] A. Sedhain, J. Li, J. Y. Lin, and H. X. Jiang, Appl. Phys. Lett. **95**, 061106 (2009).

[21] N. Pantha, R. Dahal, M. L. Nakarmi, N. Nepal, J. Li, J. Y. Lin, and H. X. Jiang, Appl. Phys. Lett. **90**, 241101 (2007).

[22] M. Follstaedt, N. A. Missert, D. D. Koleske, C. C. Mitchell, and K. C. Cross, Appl. Phys. Lett. **83**, 4797 (2003).

[23] F. A. Ponce, D. Cherns, W. T. Young, and J. W. Steeds, Appl. Phys. Lett. **69**, 770 (1996).

[24] P. B. Hirsch, A. Howie, R. B. Nicholson, D. W. Pashley, and M. J. Whelan, Electron Microscopy of Thin Crystals (Krieger, New York, 1977).

[25] S. Srinivasan, L. Geng, R. Liu, and F. A. Ponce, Appl. Phys. Lett. **83**, 5187 (2003).

[26] S. R. Lee, A. M. West, A. A. Allerman, K. E. Waldrip, D. M. Follstaedt, P. P. Provencio, D. D. Koleske, and C. R. Abernathy, Appl. Phys. Lett. **86**, 241904 (2005).

[27] K. Dovidenko, S. Oktyabrsy, and J. Narayan, J. Appl. Phys. **82**, 4296 (1997).

[28] J. Bai, T. Wang, P. J. Parbrook, K. B. Lee, and A. G. Cullis, J. Cryst. Growth **282**, 290 (2005).

[29] H. Klapper, Mater. Chem. Phys. **66**, 101 (2000).